Current Biology, Vol. 12, 648–653, April 16, 2002, ©2002 Elsevier Science Ltd. All rights reserved. PII S0960-9822(02)00763-7

A Murine Model of Nijmegen Breakage Syndrome

Bret R. Williams,[1,2] Olga K. Mirzoeva,[1] William F. Morgan,[3] Junyu Lin,[1] Wesley Dunnick,[4] and John H.J. Petrini[1,2,5]

[1]Laboratory of Genetics
University of Wisconsin Medical School
[2]Program in Cellular and Molecular Biology
University of Wisconsin
Madison, Wisconsin 53706
[3]The Radiation Oncology Research Laboratory
University of Maryland School of Medicine
Baltimore, Maryland 21201
[4]Department of Microbiology and Immunology
University of Michigan Medical School
Ann Arbor, Michigan 48109-0620

Summary

Nijmegen breakage syndrome (NBS) is a rare autosomal recessive disorder characterized by microcephaly, immunodeficiency, and predisposition to hematopoietic malignancy [1]. The clinical and cellular phenotypes of NBS substantially overlap those of ataxia-telangiectasia (A-T). NBS is caused by mutation of the *NBS1* gene, which encodes a member of the Mre11 complex [2, 3], a trimeric protein complex also containing Mre11 and Rad50 [4]. Several lines of evidence indicate that the ataxia-telangiectasia mutated (ATM) kinase and the Mre11 complex functionally interact [5]. Both NBS and A-T cells exhibit ionizing radiation (IR) sensitivity and defects in the intra S phase checkpoint, resulting in radioresistant DNA synthesis (RDS)—the failure to suppress DNA replication origin firing after IR exposure [6]. NBS1 is phosphorylated by ATM in response to IR, and this event is required for activation of the intra S phase checkpoint (the RDS checkpoint) [7–10]. We derived a murine model of NBS, the *Nbs1*$^{\Delta B/\Delta B}$ mouse. *Nbs1*$^{\Delta B/\Delta B}$ cells are phenotypically identical to those established from NBS patients. The Nbs1$^{\Delta B}$ allele was synthetically lethal with ATM deficiency. We propose that the ATM-Mre11 complex DNA damage response pathway is essential and that ATM or the Mre11 complex serves as a nexus to additional components of the pathway.

Results and Discussion

Derivation of *Nbs1*$^{\Delta B/\Delta B}$ Mice

The 657del5 allele found in 95% of NBS patients encodes two NBS1 protein species, a 26 kDa moiety that includes amino acids 1 to 218, and a 70 kDa species, NBS1^{p70}, which contains the NBS1 C terminus and thereby interacts with Mre11 [1, 11]. To model NBS in the mouse, a hypomorphic *Nbs1* mutant mouse was derived in which *NBS1* exons 4 and 5 are replaced by *neo* in the *Nbs1*$^{\Delta B}$ targeted locus, deleting the BRCT domain [2] (Figure 1A).

The *Nbs1*$^{\Delta B}$ allele produced an 80 kDa Nbs1 protein species, Nbs1^{p80}, which coimmunoprecipitates with Mre11 (Figure 1B). The mRNA encoding Nbs1^{p80} originated in the multiple cloning site flanking the *neo* marker and contained 108 bp of intronic sequences (Figure 1C) spliced to exon 6. Nbs1^{p80} immunoprecipitates were reactive with antiserum recongnizing the intron-encoded amino acids but not with N-terminal-specific Nbs1 antiserum (Figures 1B and 1D). Hence, like NBS1^{p70}, Nbs1^{p80} lacks the FHA and BRCT domains encoded in exons 1 through 5 and is capable of interaction with Mre11 [2, 11, 12]. The protein Nbs1^{p80} is thus identical to NBS1^{p70} in all but the N-terminal 66 amino acids (Figure 1E).

Nbs1$^{\Delta B/\Delta B}$ Phenotypic Outcomes Recapitulate NBS

In contrast to null *Nbs1* mutants [13], homozygous *Nbs1*$^{\Delta B/\Delta B}$ cells and mice were viable. Cells established from *Nbs1*$^{\Delta B/\Delta B}$ mice were examined to determine whether the *Nbs1*$^{\Delta B}$ allele recapitulated the cellular phenotypes of NBS. SV40 transformed *Nbs1*$^{\Delta B/\Delta B}$ murine embryonic fibroblasts (MEFs), ND7, and 54-4 exhibited pronounced sensitivity to IR (Figure 2A) and the interstrand crosslinking agent mitomycin C (data not shown). DNA synthesis rates were significantly higher in irradiated *Nbs1*$^{\Delta B/\Delta B}$ MEFs than wild-type control MEFs 60 min after IR treatment (10 Gy $p \leq 0.0003$, 20 Gy $p \leq 7 \times 10^{-5}$, Poisson) (Figure 2B), indicating that the intra S phase checkpoint is defective in *Nbs1*$^{\Delta B/\Delta B}$ cells. As in NBS cells [3, 14], these phenotypic outcomes were associated with failure to form IR-induced Mre11 and Nbs1 foci and mislocalization of the Mre11 complex in unirradiated cells (Figure 2C). The yield of chromosome aberrations following IR treatment was significantly higher in *Nbs1*$^{\Delta B/\Delta B}$ than wild-type primary MEFs, exhibiting increases in both deletion and exchange type aberrations (Figure 2D).

Conflicting data regarding the influence of Nbs1 on p53 and its associated DNA damage-dependent checkpoints have been reported [15–19]. We examined changes in the p53 transcriptional target p21 following IR treatment of primary MEFs. p21 induction was maximal by 2 hr post IR in *Nbs1*$^{\Delta B/\Delta B}$ MEFs as well as wild-type MEFs (Figure 3A, 2 hr). These data support the interpretation that inappropriate regulation of p53 is not relevant to the pathology observed in NBS patients [3, 19].

ATM also regulates the initiation of mitosis in clastogen-treated cells, although data from human lymphoblastoid cells regarding the role of Nbs1 in the G2/M checkpoint are conflicting [20, 21]. The G2/M checkpoint was analyzed in primary *Nbs1*$^{\Delta B/\Delta B}$ MEFs by measuring the abundance of phosphorylated histone H3, which marks cells in mitosis, 60 min after IR treatment. The mitotic index of wild-type MEF cultures was reduced by 15-fold (from 0.6% to 0.04%) upon IR treatment, whereas the change in two independent *Nbs1*$^{\Delta B/\Delta B}$ primary MEF cultures was ~1.7-fold, changing from 0.7%

[5]Correspondence: jpetrini@facstaff.wisc.edu

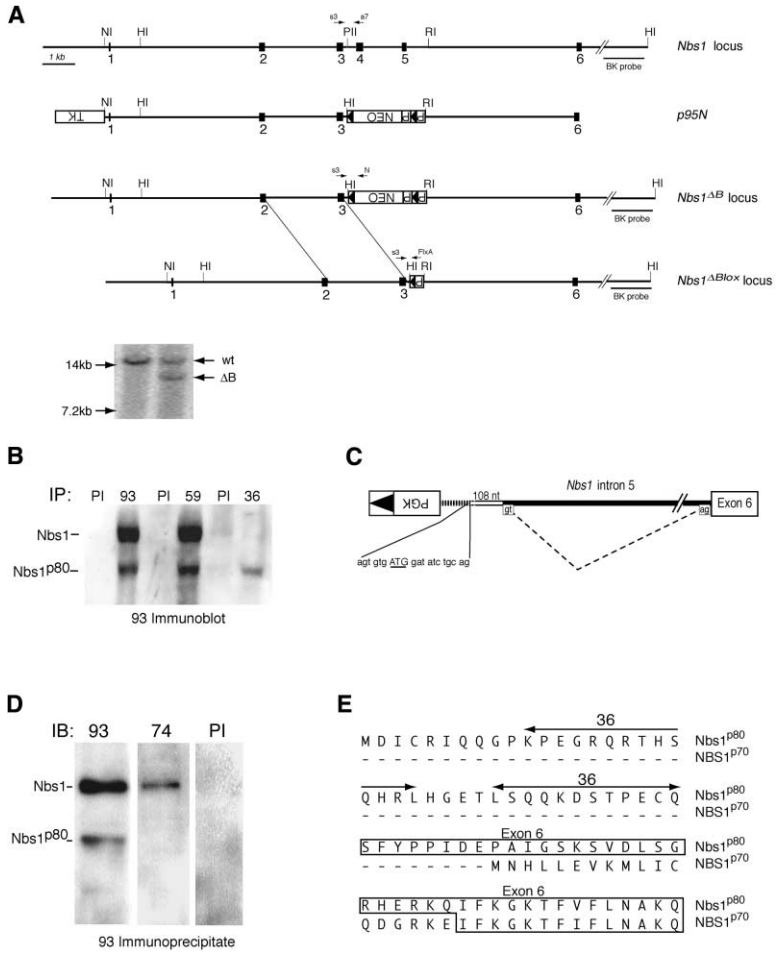

Figure 1. Creation of *Nbs1*$^{\Delta B}$ Targeting Vector and Characterization of Nbs1^{p80}

(A) Structure of *Nbs1* locus and targeting vector *p95N* as well as the product of the targeted homologous recombination event and removal of the *PGK-neo* cassette by the expression of *cre* recombinase are shown. Transcriptional orientation of *neo* is opposite to that of *Nbs1*. Targeted clones were identified using a 3′ external probe (BK), which detects the change of a 14 kb wild-type BamHI fragment into a novel 8 kb BamHI fragment. In the *cre*-mediated excision, the 8 kb BamHI fragment is reduced to 6 kb. The primers indicated by arrows enable PCR identification of the wild-type (s3 + a7) and *Nbs1*$^{\Delta B}$ (s3 + N) as well as *Nbs1*$^{\Delta Blox}$ (s3 + FlxA). Inset shows representative Southern blot identification of a targeted clone. BamHI digest from wild-type (wt) and one targeted clone (ΔB) detected with BK probe are indicated. Restriction sites noted: NcoI, NI; BamHI, HI; PvuII, PII; EcoRI, RI. Introns in thin black. Exons denoted by black boxes. Filled triangles, *loxP* sites; TK, *HSVtk* cassette; P, *PGK* promoter.

(B) Immunoprecipitation from *Nbs1*$^{+/\Delta B}$ ES cell extracts was carried out with antisera to Nbs1 (93), Mre11(59), intron 5 peptide sequences (36), or corresponding preimmune and then subjected to Western blot analysis Nbs1 (93) antiserum.

(C) The *Nbs1*^{p80} mRNA contains sequence from the multiple cloning site (hatched line) present in the targeting vector flanking the *PGK-neo* cassette followed by 108 nucleotides of intron 5 (open box) which are spliced to exon 6 to produce Nbs1^{p80} mRNA. The remainder of intron 5 is indicated by black box. The presumptive translation initiation site, present in multiple cloning site sequence, is underlined. Splice donor (gt) and acceptor (ag) sites present in intron 5 are boxed. Dashed line represents the splicing event. PGK indicates the location of the *PGK* promoter. Black triangle indicates the *loxP* site.

(D) Immunoprecipitation from *Nbs1*$^{+/\Delta B}$ ES cell extracts was carried out with Nbs1 antiserum (93) and blotted with Nbs1 (93), N-terminal-specific Nbs1 (74), or its preimmune antiserum (PI). Nbs1^{p80} does not contain sequences in exons 1 through 5.

(E) Nbs1^{p80} is similar to the protein produced from the 657del5 *NBS1* allele. Nbs1^{p80} is identical to endogenous Nbs1^{p95} beginning with exon 6 (boxed). NBS1^{p70} exhibits identity with Nbs1^{p95} in the middle of exon 6, downstream of the 657del5 mutation [11]. Peptides used to derive intron 5-specific antiserum (36) are shown.

to 0.4% and 0.6% to 0.4% ($p \leq 2.76 \times 10^{-21}$, χ^2) (Figure 3B). These data indicate that Nbs1 (and, by extension, the Mre11 complex) influence both the RDS and G2/M checkpoints in murine cells.

Phenotypic Features of *Nbs1*$^{\Delta B/\Delta B}$ Mice

Although the phenotypic features of *Nbs1*$^{\Delta B/\Delta B}$ MEFs recapitulated those observed in NBS cells, certain aspects of the organismal phenotypes of *Nbs1*$^{\Delta B/\Delta B}$ mice were less severe than those of NBS patients. NBS patients exhibit immune system defects, most commonly manifest as IgG or IgA deficiency (49/55 patients). Immunoglobulin isotype profiles of *Nbs1*$^{\Delta B/\Delta B}$ mice (aged 3–6.8 month) were indistinguishable from normal controls, and flow cytometric analyses indicated that splenic B and thymic T cell populations in *Nbs1*$^{\Delta B/\Delta B}$ mice varied by less than 25% from those in wild-type controls (data not shown).

Though five of the 55 patients in the NBS registry exhibited ovarian dysgenesis, delayed or aberrant development of secondary sexual characteristics are not commonly observed features of NBS patients [1]. Consistent with this aspect of the NBS clinical picture, *Nbs1*$^{\Delta B/\Delta B}$ males and females were fertile, and histological analyses reavealed no abnormalities in ovaries or testes (data not shown).

Nbs1$^{\Delta B/\Delta B}$ mice were not markedly prone to malignancy. Tumor incidence in an aged population of 36 *Nbs1*$^{\Delta B/\Delta B}$ mice was not significantly higher than in heterozygous and wild-type control populations (Figure 4A). This number of mice was sufficient to establish a 2-fold increase in tumor incidence with 95% confidence; the data do not preclude a more subtle effect. Given the DNA damage response defects in *Nbs1*$^{\Delta B/\Delta B}$ MEFs, we reasoned that the *Nbs1*$^{\Delta B}$ mutation would affect the metabolism of intrinsic DNA damage and enhance the tumor predisposition of p53-deficient mice [22]. *p53*$^{-/-}$ and *Nbs1*$^{\Delta B/+}$ *p53*$^{-/-}$ exibited a similar tumor latency, indicating that *Nbs1*$^{\Delta B/\Delta B}$ was recessive. However, tu-

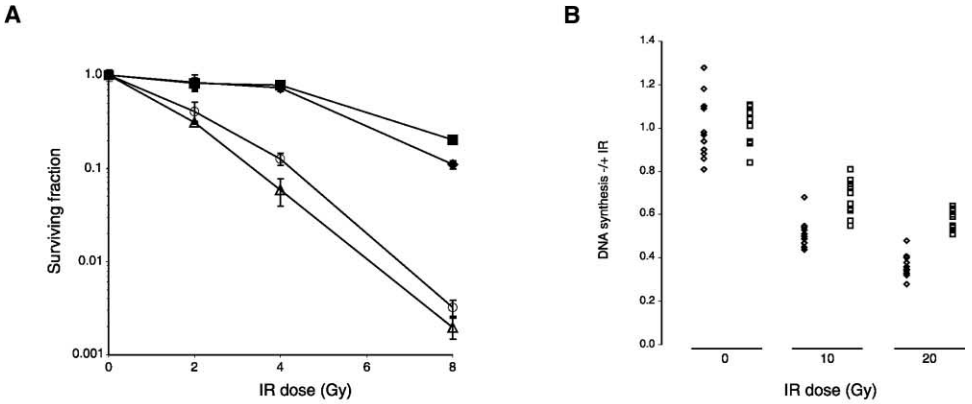

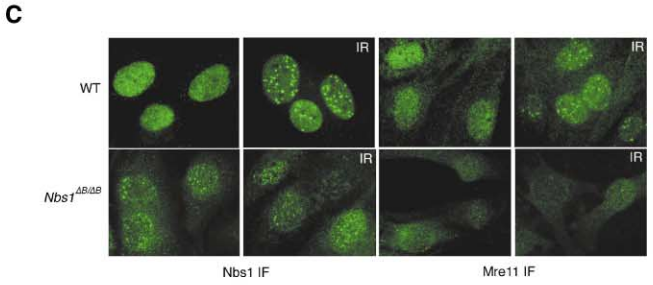

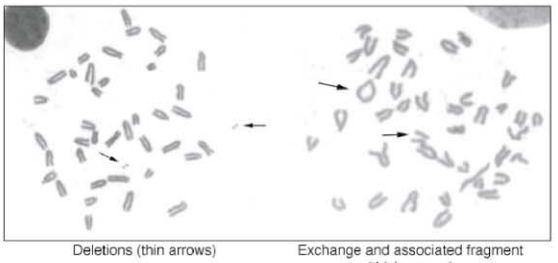

Dose (Gy)	% aberrant metaphases	Exchanges	Deletions
WT			
0	0	0	0
0.5	12	2	11
1.0	22	7	17
2.5	39	19	32
Nbs1ΔB/ΔB			
0	0	0	0
0.5	25	4	26
1.0	38	14	40
2.5	60	31	59

Figure 2. *Nbs1*$^{\Delta B/\Delta B}$ Fibroblasts Recapitulate the Cellular Phenotypes of NBS

(A) *Nbs1*$^{\Delta B/\Delta B}$ cells are radiosensitive. IR sensitivity was determined by colony formation assay. Two wild-type, ND4 (closed diamonds) and 54-5 (closed squares), and two *Nbs1*$^{\Delta B/\Delta B}$, ND7 (open triangles) and 54-4 (open circles), are plotted for each dose. Data shown are the result of a representative experiment done in triplicate for each genotype at doses indicated. Colony number is normalized to untreated plates to account for plating efficiency. Error bars indicate standard deviation.

(B) *Nbs1*$^{\Delta B/\Delta B}$ display radioresistant DNA synthesis. DNA synthesis rates in wild-type (ND4 and 54-5, open diamonds) and *Nbs1*$^{\Delta B/\Delta B}$ (ND7 and 54-4, open squares) graphed together by genotype. [^{14}C]thymidine-labeled cells are treated with ionizing radiation, and levels of DNA synthesis are determined 1 hr postirradiation by incorporation of [^{3}H]thymidine. Ratios of [^{3}H] to [^{14}C] are determined and normalized to the untreated samples. This plot shows a representative plot of two separate experiments, and each symbol represents an independent culture.

(C) *Nbs1*$^{\Delta B/\Delta B}$ cells are defective in the formation of ionizing radiation induced foci (IRIF). Primary wild-type (WT) and *Nbs1*$^{\Delta B/\Delta B}$ cells were stained for Mre11 (Mre11 IF) and Nbs1 (Nbs1 IF) after mock treatment or 8 hr post IR (IR). Note the increase in cytoplasmic staining and lack of IRIF formation as in NBS fibroblasts.

(D) *Nbs1*$^{\Delta B/\Delta B}$ cells display increased chromosomal aberrations after treatment with IR. Exponentially growing primary MEF cultures were treated with increasing X-ray doses, and metaphase spreads were prepared for analysis of aberrations. Aberrations shown are representative of those quantitated in the table. Exchange and reciprocal fragments arise from assymetric recombination between two chromosomes. The irradiation protocol employed biases for G1 events. Hence, the yield of chromatid aberrations was extremely low relative to chromosome breaks.

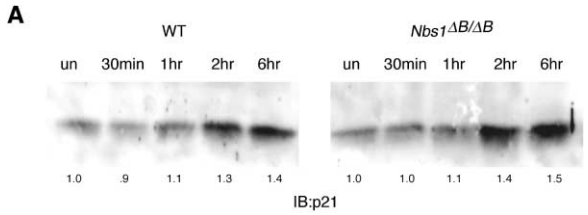

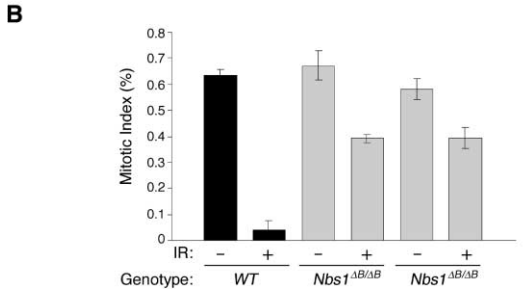

Figure 3. Cell Cycle Checkpoint Activation in *Nbs1*$^{\Delta B/\Delta B}$ Fibroblasts

(A) *Nbs1*$^{\Delta B/\Delta B}$ cells have a normal p21 response. Extracts of wild-type (WT) and *Nbs1*$^{\Delta B/\Delta B}$ primary MEF cultures were prepared at the indicated times after IR treatment. p21 levels were assessed by Western blotting. Equivalent loading, determined by Bradford assay, were verified by quantitative comparison to a nonspecific band as well as to β-actin (data not shown). Ratios of p21 to the nonspecific band as determined by Storm scanning are shown beneath each lane.

(B) *Nbs1*$^{\Delta B/\Delta B}$ cells exhibit a G2/M checkpoint defect. Exponentially growing wild-type (WT) and *Nbs1*$^{\Delta B/\Delta B}$ primary MEF cultures were treated with 10 Gy IR and harvested at 1 hr posttreatment. Cells were stained with a histone-H3 phosphospecific antiserum to identify cells in mitosis and were scored by FACS. Graph shown is from a representative experiment; each treatment was performed in triplicate, and at least 10,000 events per sample were counted. Mitotic index is the percentage of mitotic cells in the irradiated culture. Error bars indicate standard deviation.

mors arose in *Nbs1*$^{\Delta B/\Delta B}$ *p53*$^{-/-}$ mice significantly earlier than in *p53*$^{-/-}$ mice ($p \leq 0.004$, Poisson) (Figure 4B). These observations implied that the *Nbs1*$^{\Delta B}$ mutation was associated with the accumulation of potentially oncogenic genetic alterations and that lack of cancer predisposition in *Nbs1*$^{\Delta B/\Delta B}$ mice was attributable to suppression by p53.

Synthetic Lethality of *Nbs1*$^{\Delta B}$ and *Atm* Mutations

Atm$^{-/-}$ mice recapitulate several aspects of A-T, including defects in the RDS [23] and G2/M checkpoints (C.F. Bender and J.H.J.P., unpublished data), defects also observed in *Nbs1*$^{\Delta B/\Delta B}$ mice. In human cells, Nbs1 and ATM interact in both RDS and G2/M checkpoint functions. Therefore, we hypothesized that Atm deficiency would be epistatic to the *Nbs1*$^{\Delta B}$ mutation. *Nbs1*$^{\Delta B/\Delta B}$ mice were crossed with *Atm* (*Atm*$^{-/+}$) mice. Whereas *Nbs1*$^{\Delta B/\Delta B}$ mice were obtained at normal Mendelian frequencies, *Nbs1*$^{\Delta B/\Delta B}$ *Atm*$^{-/-}$ mice were not obtained from either *Nbs1*$^{\Delta B/+}$ *Atm*$^{-/+}$ or *Nbs1*$^{\Delta B/\Delta B}$ *Atm*$^{-/+}$ intercrosses ($p \leq 7.09 \times 10^{-23}$, Poisson) (Figure 4C). The synthetic lethality of *Nbs1*$^{\Delta B}$ with *Atm*$^{-/-}$ was manifest early in embryogenesis, as no double mutant embryos were detected at embryonic day 10 ($p \leq 0.006$, Poisson) (Figure 4C).

A parsimonious interpretation of *Nbs1*$^{\Delta B/\Delta B}$ *Atm*$^{-/-}$ synthetic lethality is that the effects of each mutation are additive. Inefficient metabolism of chromosomal lesions combined with the attenuation of checkpoint responses may be inconsistent with viability of the developing embryo. Whereas the decreased latency tumor latency in *Nbs1*$^{\Delta B/\Delta B}$ *p53*$^{-/-}$ mice supports this interpretation, the lack of gross karyotypic instability in *Nbs1*$^{\Delta B/\Delta B}$ *p53*$^{-/-}$ thymic lymphomas and MEFs (data not shown) would appear to undermine it. However, rate of chromosome breakage and metabolism in those cell types may not be comparable to that in rapidly dividing embryonic cells.

Nbs1^{p70} phosphorylation is not impaired in NBS cells, suggesting that physical interaction between ATM and Mre11 complex is not abrogated in NBS cells or *Nbs1*$^{\Delta B/\Delta B}$ mice [11]. Hence, an alternative interpretation

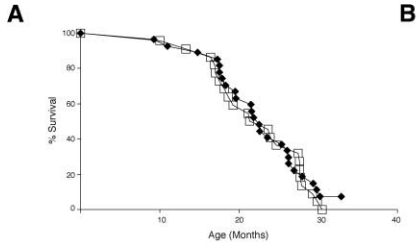

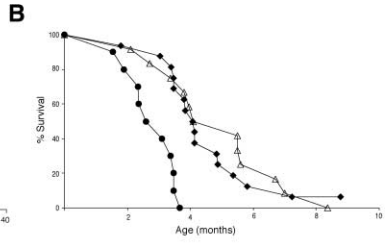

C

Age	Genotype	Observed	Expected
Weaning			
	Nbs1$^{+/+}$ *Atm*$^{-/-}$	20	15
	Nbs1$^{+/\Delta B}$ *Atm*$^{-/-}$	62	67
	Nbs1$^{\Delta B/\Delta B}$ *Atm*$^{-/-}$	0	51
10dpc			
	Nbs1$^{+/+}$ *Atm*$^{-/-}$	1	2
	Nbs1$^{+/\Delta B}$ *Atm*$^{-/-}$	4	7
	Nbs1$^{\Delta B/\Delta B}$ *Atm*$^{-/-}$	0	5

Figure 4. Survival and Genetic Interactions of *Nbs1*$^{\Delta B/\Delta B}$ Mice

(A) Survival of *Nbs1*$^{\Delta B/\Delta B}$ mice. Survival of wild-type mice (closed diamonds) and *Nbs1*$^{\Delta B/\Delta B}$ mice (open squares) was determined. Percent survival is plotted as a function of age.

(B) Survival of *Nbs1/p53* mice. Twelve *p53*$^{-/-}$ (open triangles), sixteen *Nbs1*$^{+/\Delta B}$ *p53*$^{-/-}$ (closed diamonds), and ten *Nbs1*$^{\Delta B/\Delta B}$ *p53*$^{-/-}$ (closed circles) were monitored for signs of morbidity. Tumor latency is significantly shorter in *Nbs1*$^{\Delta B/\Delta B}$ *p53*$^{-/-}$ ($p \leq 0.004$, Poisson), although tumor spectrum is not different than that of *p53*$^{-/-}$ alone [22]. Out of ten *Nbs1*$^{\Delta B/\Delta B}$ *p53*$^{-/-}$ animals monitored, six lymphomas and two teratomas were observed. Percent survival is plotted as a function of age.

(C) Embryonic lethality of *Nbs1*$^{\Delta B/\Delta B}$ *Atm*$^{-/-}$ mice. Animals were crossed to assess the viability of *Nbs1*$^{\Delta B/\Delta B}$ *Atm*$^{-/-}$ animals. For weaning, the genotype of offspring present 21days after birth was determined ($p \leq 7.09 \times 10^{-23}$, Poisson). Early embryonic lethality was determined by sacrificing females with the subsequent genotyping of observed embryos 10 days post coitus (dpc) ($p \leq 0.006$, Poisson).

is that protein interactions at the FHA and BRCT domains at the N terminus of Nbs1 are essential for viability in the absence of ATM; such interactions would be abrogated in *Nbs1*$^{\Delta B/\Delta B}$ mice and physically uncoupled from the Mre11 complex in NBS cells. Candidate interacting proteins are E2F1 and 2, which we have previously demonstrated interact with the Nbs1 N terminus [24]. *Nbs1*$^{\Delta B/\Delta B}$ *E2F1*$^{-/-}$ and *Atm*$^{-/-}$ *E2F1*$^{-/-}$ are viable (B.R.W. and J.H.J.P., unpublished data), although this may be attributable to redundancy of E2F1 and E2F2. In addition, it is conceivable that the Mre11 complex and ATR functionally interact, since ATR has been implicated in both the RDS and G2/M checkpoints [25–28]. In such a scenario, ATR and ATM would both regulate the Mre11 complex in wild-type cells, but the ATR-dependent functions would be compromised in *Nbs1*$^{\Delta B/\Delta B}$ and, by extension, NBS cells, whereas some of the ATM-regulated functions would be retained. In the context of Atm deficiency, the residual functions of the Mre11 complex would be further compromised and result in lethality.

Supplementary Material

Supplementary Material including additional methodological details can be found at http://images.cellpress.com/supmat/supmatin.htm.

Acknowledgments

The authors are grateful to Jennifer Salna for animal care and management; Carla Bender and Takehiko Usui for critical reading of the manuscript; members of the Petrini lab, Eugene Oltz and David Roth for helpful discussion; Norman Drinkwater for statistical advice; the Perry and Lambert labs for reagents and advice; and Yang Xu for sharing unpublished data. This work was supported by National Institutes of Health grants GM59413 (J.H.J.P), CA39068 (W.A.D.), the Biological and Environmental Research Program (BER) U.S. Department of Energy, Grant Number DE-FG02-99ER62859 (J.H.J.P. and W.F.M.), NIH predoctoral training grant 5T32GM07133, and the Mouse Model of Human Cancer Consortium Grant 5 U01 CA84227-03 (B.R.W.). Manuscript #3593 from the University of Wisconsin Laboratory of Genetics.

Received: December 21, 2001
Revised: February 1, 2002
Accepted: February 5, 2002
Published: April 16, 2002

References

1. Group TINBSS. (2000). Nijmegen breakage syndrome. Arch. Dis. Child. *82*, 400–406.
2. Varon, R., Vissinga, C., Platzer, M., Cerosaletti, K.M., Chrzanowska, K.H., Saar, K., Beckmann, G., Seemanova, E., Cooper, P.R., Nowak, N.J., et al. (1998). Nibrin, a novel DNA double-strand break repair protein, is mutated in Nijmegen breakage syndrome. Cell *93*, 467–476.
3. Carney, J.P., Maser, R.S., Olivares, H., Davis, E.M., Le Beau, M., Yates, J.R., III, Hays, L., Morgan, W.F., and Petrini, J.H.J. (1998). The hMre11/hRad50 protein complex and Nijmegen breakage syndrome: linkage of double-strand break repair to the cellular DNA damage response. Cell *93*, 477–486.
4. Maser, R.S., Bressan, D.A., and Petrini, J.H.J. (2001). The Mre11-Rad50 complex: diverse functions in the cellular DNA damage response. In DNA Damage and Repair, Volume 3, M.F. Hoekstra and J.A. Nickoloff, eds. (Totowa, NJ: Humana Press), pp. 147–172.
5. Petrini, J.H. (2000). The mre11 complex and ATM: collaborating to navigate S phase. Curr. Opin. Cell Biol. *12*, 293–296.
6. Shiloh, Y. (1997). Ataxia-telangiectasia and the Nijmegen breakage syndrome: related disorders but genes apart. Annu. Rev. Genet. *31*, 635–662.
7. Gatei, M., Young, D., Cerosaletti, K.M., Desai-Mehta, A., Spring, K., Kozlov, S., Lavin, M.F., Gatti, R.A., Concannon, P., and Khanna, K. (2000). ATM-dependent phosphorylation of nibrin in response to radiation exposure. Nat. Genet. *25*, 115–119.
8. Zhao, S., Weng, Y.C., Yuan, S.S., Lin, Y.T., Hsu, H.C., Lin, S.C., Gerbino, E., Song, M.H., Zdzienicka, M.Z., Gatti, R.A., et al. (2000). Functional link between ataxia-telangiectasia and Nijmegen breakage syndrome gene products. Nature *405*, 473–477.
9. Wu, X., Ranganathan, V., Weisman, D.S., Heine, W.F., Ciccone, D.N., O'Neill, T.B., Crick, K.E., Pierce, K.A., Lane, W.S., Rathbun, G., et al. (2000). ATM phosphorylation of Nijmegen breakage syndrome protein is required in a DNA damage response. Nature *405*, 477–482.
10. Lim, D.S., Kim, S.T., Xu, B., Maser, R.S., Lin, J., Petrini, J.H.J., and Kastan, M.B. (2000). ATM phosphorylates p95/Nbs1 in an S-phase checkpoint pathway. Nature *404*, 613–617.
11. Maser, R.S., Zinkel, R., and Petrini, J.H.J. (2001). An alternative mode of translation permits production of a variant NBS1 protein from the common Nijmegen breakage syndrome allele. Nat. Genet. *27*, 417–421.
12. Vissinga, C.S., Yeo, T.C., Woessner, J., Massa, H.F., Wilson, R.K., Trask, B.J., and Concannon, P. (1999). Identification, characterization, and mapping of a mouse homolog of the gene mutated in Nijmegen breakage syndrome. Cytogenet. Cell Genet. *87*, 80–84.
13. Zhu, J., Petersen, S., Tessarollo, L., and Nussenzweig, A. (2001). Targeted disruption of the Nijmegen breakage syndrome gene NBS1 leads to early embryonic lethality in mice. Curr. Biol. *11*, 105–109.
14. Desai-Mehta, A., Cerosaletti, K.M., and Concannon, P. (2001). Distinct functional domains of nibrin mediate Mre11 binding, focus formation, and nuclear localization. Mol. Cell. Biol. *21*, 2184–2191.
15. Jongmans, W., Vuillaume, M., Chrzanowska, K., Smeets, D., Sperling, K., and Hall, J. (1997). Nijmegen breakage syndrome cells fail to induce the p53-mediated DNA damage response following exposure to ionizing radiation. Mol. Cell. Biol. *17*, 5016–5022.
16. Matsuura, K., Balmukhanov, T., Tauchi, H., Weemaes, C., Smeets, D., Chrzanowska, K., Endou, S., Matsuura, S., and Komatsu, K. (1998). Radiation induction of p53 in cells from Nijmegen breakage syndrome is defective but not similar to ataxia-telangiectasia. Biochem. Biophys. Res. Commun. *242*, 602–607.
17. Yamazaki, V., Wegner, R.D., and Kirchgessner, C.U. (1998). Characterization of cell cycle checkpoint responses after ionizing radiation in Nijmegen breakage syndrome cells. Cancer Res. *58*, 2316–2322.
18. Sullivan, K.E., Veksler, E., Lederman, H., and Lees-Miller, S.P. (1997). Cell cycle checkpoints and DNA repair in Nijmegen breakage syndrome. Clin. Immunol. Immunopathol. *82*, 43–48.
19. Stewart, G., Maser, R.S., Stankovic, T., Bressan, D.A., Kaplan, M.I., Jaspers, N.G.J., Byrd, P.J., Petrini, J.H.J., and Taylor, A.M.R. (1999). The DNA double strand break repair gene hMre11 is mutated in individuals with a new ataxia telangiectasia like disorder (ATLD). Cell *99*, 577–587.
20. Xu, B., Kim, S., and Kastan, M.B. (2001). Involvement of Brca1 in S-phase and G(2)-phase checkpoints after ionizing irradiation. Mol. Cell. Biol. *21*, 3445–3450.
21. Buscemi, G., Savio, C., Zannini, L., Micciche, F., Masnada, D., Nakanishi, M., Tauchi, H., Komatsu, K., Mizutani, S., Khanna, K., et al. (2001). Chk2 activation dependence on Nbs1 after DNA damage. Mol. Cell. Biol. *21*, 5214–5222.
22. Jacks, T., Remington, L., Williams, B.O., Schmitt, E.M., Halachmi, S., Bronson, R.T., and Weinberg, R.A. (1994). Tumor spectrum analysis in p53-mutant mice. Curr. Biol. *4*, 1–7.
23. Barlow, C., Hirotsune, S., Paylor, R., Liyanage, M., Eckhaus, M., Collins, F., Shiloh, Y., Crawley, J.N., Ried, T., Tagle, D., et al. (1996). Atm-deficient mice: a paradigm of ataxia telangiectasia. Cell *86*, 159–171.
24. Maser, R.S., Mirzoeva, O.K., Wells, J., Olivares, H., Williams, B.R., Zinkel, R., Farnham, P.J., and Petrini, J.H.J. (2001). The MRE11 complex and DNA replication: linkage to E2F and sites of DNA synthesis. Mol. Cell. Biol. *21*, 6006–6016.

25. Cliby, W.A., Roberts, C.J., Cimprich, K.A., Stringer, C.M., Lamb, J.R., Schreiber, S.L., and Friend, S.H. (1998). Overexpression of a kinase-inactive ATR protein causes sensitivity to DNA-damaging agents and defects in cell cycle checkpoints. EMBO J. *17*, 159–169.
26. Bao, S., Tibbetts, R.S., Brumbaugh, K.M., Fang, Y., Richardson, D.A., Ali, A., Chen, S.M., Abraham, R.T., and Wang, X.F. (2001). ATR/ATM-mediated phosphorylation of human Rad17 is required for genotoxic stress responses. Nature *411*, 969–974.
27. Tibbetts, R.S., Cortez, D., Brumbaugh, K.M., Scully, R., Livingston, D., Elledge, S.J., and Abraham, R.T. (2000). Functional interactions between BRCA1 and the checkpoint kinase ATR during genotoxic stress. Genes Dev. *14*, 2989–3002.
28. Cortez, D., Guntuku, S., Qin, J., and Elledge, S.J. (2001). ATR and ATRIP: partners in checkpoint signaling. Science *294*, 1713–1716.